



Bio-ink development for three-dimensional bioprinting of hetero-cellular cartilage constructs

Vivian H. M. Mouser, Riccardo Levato, Anneloes Mensinga, Wouter J. A. Dhert, Debby Gawlitta & Jos Malda

To cite this article: Vivian H. M. Mouser, Riccardo Levato, Anneloes Mensinga, Wouter J. A. Dhert, Debby Gawlitta & Jos Malda (2020) Bio-ink development for three-dimensional bioprinting of hetero-cellular cartilage constructs, *Connective Tissue Research*, 61:2, 137-151, DOI: [10.1080/03008207.2018.1553960](https://doi.org/10.1080/03008207.2018.1553960)

To link to this article: <https://doi.org/10.1080/03008207.2018.1553960>



© 2018 The Author(s). Published by Informa UK Limited, trading as Taylor & Francis Group.



[View supplementary material](#)



Published online: 10 Dec 2018.



[Submit your article to this journal](#)



Article views: 2591



[View related articles](#)



[View Crossmark data](#)



Citing articles: 23 [View citing articles](#)

Bio-ink development for three-dimensional bioprinting of hetero-cellular cartilage constructs

Vivian H. M. Mouser^a, Riccardo Levato^a, Anneloes Mensinga^a, Wouter J. A. Dhert^b, Debby Gawlitta^c, and Jos Malda^{a,b}

^aDepartment of Orthopaedics, University Medical Center Utrecht, Utrecht University, Utrecht, The Netherlands; ^bDepartment of Equine Sciences, Faculty of Veterinary Medicine, Utrecht University, Utrecht, The Netherlands; ^cDepartment of Oral and Maxillofacial Surgery & Special Dental Care, University Medical Center Utrecht, Utrecht University, Utrecht, The Netherlands

ABSTRACT

Bioprinting is a promising tool to fabricate organized cartilage. This study aimed to investigate the printability of gelatin-methacryloyl/gellan gum (gelMA/gellan) hydrogels with and without methacrylated hyaluronic acid (HAMA), and to explore (zone-specific) chondrogenesis of chondrocytes, articular cartilage progenitor cells (ACPCs), and multipotent mesenchymal stromal cells (MSCs) embedded in these bio-inks.

The incorporating of HAMA in gelMA/gellan bio-ink increased filament stability, as measured using a filament collapse assay, but did not influence (zone-specific) chondrogenesis of any of the cell types. Highest chondrogenic potential was observed for MSCs, followed by ACPCs, which displayed relatively high proteoglycan IV mRNA levels. Therefore, two-zone constructs were printed with gelMA/gellan/HAMA containing ACPCs in the superficial region and MSCs in the middle/deep region. Chondrogenic differentiation was confirmed, however, printing influence cellular differentiation.

ACPC- and MSC-laden gelMA/gellan/HAMA hydrogels are of interest for the fabrication of cartilage constructs. Nevertheless, this study underscores the need for careful evaluation of the effects of printing on cellular differentiation.

ARTICLE HISTORY

Received 16 August 2018
Revised 5 October 2018
Accepted 12 November 2018

KEYWORDS



Chondroprogenitor cells; GelMA/gellan; hyaluronic acid; mesenchymal stromal cells; zonal cartilage


Introduction

Articular cartilage damage often results in osteoarthritic changes of the joint if no interventions are taken (1,2). Articular cartilage is the tissue covering the bone extremities and consists of predominantly water, proteoglycans, and collagen type II (2,3). The tissue contains depth-dependent characteristics and can be divided into three zones: the superficial zone (10–20%), the middle or intermediate zone (40–60%), and the deep zone (30–40%). Matrix composition, collagen orientation, and mechanical properties differ among these layers, as well as chondrocyte density (4,5). In the superficial layer, chondrocytes synthesize more proteoglycan IV (PRG4, or lubricin) (6,7), clusterin (8), and collagen type I (7) compared to chondrocytes in the other zones. Additionally, proteins, such as cartilage oligomeric protein (COMP) (9) and collagen type X (7) are predominantly synthesized by cells in the middle and deep zones. Current clinical therapies, e.g. microfracture or (matrix-induced) autologous chondrocyte implantation, result in

the formation of homogeneous (fibro)cartilage, which provides pain relief for the patient, but often fails mechanically on the long term (10,11). The implantation of tissue-engineered hydrogel constructs is a promising future approach to repair cartilage defects. Additionally, the incorporation of depth-dependent organization mimicking that of native cartilage is believed to improve construct integration in the defect site compared to traditional cartilage repair strategies, and may impact on clinical outcomes (12,13).

Bioprinting techniques are a unique tool to implement spatial variations in tissue-engineered constructs, as they enable precise control over the positioning of biomaterials and cells (14). However, the search for suitable biomaterials, the bio-inks, remains challenging. Hydrogels have been identified as the most promising materials for bioprinting as their high water content provides sustenance and easy incorporation of cells and other biological components, e.g. growth factors or proteins. However, multiple material properties identified as beneficial for the printing process, such as high

CONTACT Jos Malda  j.malda@umcutrecht.nl  Department of Orthopaedics, University Medical Center Utrecht, Heidelberglaan 100, Utrecht, CX 3584, The Netherlands

 Supplemental data for this article can be accessed [here](#).

© 2018 The Author(s). Published by Informa UK Limited, trading as Taylor & Francis Group.
This is an Open Access article distributed under the terms of the Creative Commons Attribution-NonCommercial-NoDerivatives License (<http://creativecommons.org/licenses/by-nc-nd/4.0/>), which permits non-commercial re-use, distribution, and reproduction in any medium, provided the original work is properly cited, and is not altered, transformed, or built upon in any way.

polymer concentration, cross-linking density, yield stress, and viscosity, do interfere with matrix synthesis of embedded cells (15,16). A strategy to overcome this challenge involves the fine-tuning of a bio-ink with additives to generate polymer blends with both the required material properties for accurate printing and the biological properties to support matrix production and chondrogenesis of embedded cells.

A promising cartilage bio-ink consists of the collagen-derived gelatin-methacryloyl (gelMA). GelMA contains methacryloyl groups to allow UV cross-linking of the polymer chains, and was demonstrated to support cartilage-like matrix production of embedded chondrocytes and multipotent mesenchymal stromal cells (MSCs) (17–19). However, printing of gelMA is challenging as the filament stability, during printing, has to rely on the thermo-gelation behavior of gelMA, which is a relatively slow process (20,21). The printability of gelMA can be improved by the incorporation of the polysaccharide gellan gum (21). Gellan gum increases the viscosity of the gelMA/gellan blend and initiates ionic interactions. These ionic interactions induce pseudo-plastic behavior and increase the yield stress, which improves the filament stability during printing, resulting in constructs with high shape-fidelity (16,21). In addition, we recently demonstrated that the presence of relatively low gellan gum concentrations did not hamper cartilage matrix production by embedded chondrocytes, making gellan gum an interesting additive to gelMA bio-inks for cartilage bioprinting (16). Also, hyaluronic acid (HA), an element of native cartilage, has been demonstrated to improve the printability of hydrogels by increasing the viscosity of the polymer blend (22–24). In addition, HA can be methacrylated (HAMA) to allow UV cross-linking with gelMA and its presence in low concentrations was demonstrated to improve cartilage tissue formation by embedded chondrocytes (17,25). Therefore, the incorporation of HAMA in gelMA/gellan hydrogels may further improve the bio-ink properties.

Multiple cell types can be incorporated in bioprinted cartilage constructs. Most research groups focus on the incorporation of chondrocytes, as these cells already have the correct fate for cartilage formation (14). However, obtaining autologous chondrocytes can result in donor-site morbidity and chondrocyte expansion in monolayer culture stimulates chondrocyte dedifferentiation toward a fibroblastic phenotype (26). An alternative cell source is the sub-population of articular cartilage progenitor cells (ACPCs, or chondroprogenitor cells), which are mainly located in the superficial zone of articular cartilage (27,28). ACPCs allow expansion in monolayer culture without losing their

chondrogenic phenotype (27). Another alternative are MSCs, derived from, *e.g.* bone marrow, adipose tissues, or muscle (29), and thus limiting donor-site morbidity. MSCs may also be expanded in monolayer culture and can be manipulated to differentiate into chondrocyte-like cells with specific growth factors, such as the members of the transforming growth factor beta (TGF- β) superfamily (30). Thus, chondrocytes, ACPCs, and MSCs form interesting cell types for cartilage tissue-engineering purposes.

The aim of this study was to generate cartilage repair constructs that mimic the depth-dependent characteristics of the native cartilage. This requires the identification and optimization of specific bio-ink/cell-type combinations for each zone. Therefore, this study explored the suitability of two hydrogel systems, gelMA/gellan (GG) and gelMA/gellan/HAMA (GGH), for 3D printing. Additionally, chondrocytes, ACPCs, and MSCs were embedded in both bio-inks, and the production of (zone-specific) cartilage matrix was evaluated. Finally, this study explored the feasibility of obtaining a two-zone construct with zone-specific matrix production in each layer, via the bioprinting of the two optimal bio-ink/cell combinations for superficial zone cartilage and middle/deep zone cartilage.

Experimental section

Experimental design

Filament collapse, as a measure for filament stability and thus the printability, was evaluated for two gelMA-based bio-inks, gelMA/gellan (GG) and gelMA/gellan/HAMA (GGH) (Table 1), with plain gelMA (G) as a control. Next, constructs were cast using both bio-ink formulations (GG and GGH) combined with chondrocytes, ACPCs, or MSCs. The cell-laden constructs were cross-linked and cultured for 1 or 28 days to evaluate (zone-specific) cartilage matrix production and chondrogenic gene expression levels. Based on the results of the first two experiments, two-zone constructs were printed using an optimized combination of hydrogel formulation and cell type for each region (superficial and

Table 1. Overview of the polymer concentrations within the evaluated bio-ink compositions and their abbreviations. Polymer concentrations were based on previous findings (16,17,25) and all polymers were dissolved in MilliQ with 10% PBS v/v, 0.1% Irgacure, and 4.86% D-(+)-mannose.

Name	% gelMA (w/v)	% gellan gum (w/v)	% HAMA (w/v)
G	10.5	-	-
GG	10	0.5	-
GGH	9.5	0.5	0.5

middle/deep). The two-zone constructs were cultured for 1, 28, or 42 days, and samples were analyzed for (zone-specific) cartilage matrix production and chondrogenic gene expression levels.

Preparation of polymer solutions

GelMA and HAMA were synthesized from gelatin (type A from porcine skin, 175 g Bloom; degree of functionalization = 80%, Sigma Aldrich, Zwijndrecht, the Netherlands) and hyaluronic acid (120 kDa, degree of methacrylation = 10%, indicating the presence of 10 methacrylate groups for each 100 disaccharide units, Lifecore Biomedical, Chaska, USA), respectively, as previously described (21,31). GelMA, gellan gum, and HAMA stock solutions were prepared as previously described (16,24). In short, gelMA and gellan gum were dissolved at 70°C and HAMA at 4°C in Milli-Q with 10% PBS v/v, 0.1% Irgacure 2959 (gift from BASF, Ludwigshafen, Germany), and 4.86% D-(+)-mannose (Sigma Aldrich, to generate an isotonic solution). Stock solutions were stored overnight at 4°C, after which they were mixed in the correct ratio at 80°C to obtain the desired formulations (Table 1).

Screening of filament stability

The different polymer solutions were pipetted into 3-ml syringe barrels (Nordson EFD, Bedfordshire, England), which were loaded into a 3DDiscovery bioprinter (RegenHU, Villaz-St-Pierre, Switzerland). For each formulation, five filaments were printed onto substrates with aligned pillars at 1, 2, 4, 8, and 16 mm intervals, as previously described (32), using a 23-gauge metal needle (Precision Tip PN, Nordson EFD) and optimized print settings for each hydrogel formulation (Table S1). Filament deposition was recorded with a USB microscope (Bresser, Rhede, Germany) at a magnification of 20x. The average overhang the filaments reached without collapsing was determined for each formulation as a measure for filament stability.

Isolation, characterization, and expansion of cells

Chondrocytes, ACPCs, and MSCs were isolated, characterized, and expanded as previously described (16,33,34). In short, chondrocytes and ACPCs were isolated from macroscopically healthy full-thickness cartilage of equine metacarpophalangeal joints ($N = 3$ for each cell type; 3–10 years old). MSCs were isolated from bone marrow aspirates of the sternum of healthy living equine donors ($N = 3$), with approval of the local animal ethical committee. The bone marrow was

diluted in PBS, filtered through a 100- μm cell strainer, and pipetted onto a layer of Ficoll-Paque (1.077 g cm^{-3}). After centrifugation, the white mononuclear cell layer was isolated. Subsequently, the cells were washed and cultured in monolayer (seeding density of 0.25×10^6 cells cm^{-2}) with high glucose Dulbecco's modified Eagle's medium (DMEM, D6429, Sigma Aldrich) supplemented with 10% fetal bovine serum (FBS; Gibco), 1% penicillin/streptomycin (final concentration of 100 units ml^{-1} penicillin and 100 $\mu\text{g ml}^{-1}$ streptomycin), and 1 ng ml^{-1} recombinant human fibroblast growth factor-basic (bFGF, E.coli produced, R&D systems, Abingdon, UK). All cells were stored in liquid nitrogen (chondrocyte passage 0, ACPCs passage 3, MSCs passage 3) until further use.

The multipotency of the ACPCs and MSCs was previously evaluated *in vitro* with a three-way differentiation assay (34–36), as well as the expression of the characteristic cell membrane markers (34). Upon construct preparation, cells were expanded one more passage in monolayer culture as previously described to reach the desired passage (chondrocytes passage 1, ACPCs passage 4, MSCs passage 4) (16,33,34).

Construct preparation for the screening of zone-specific cartilage-like tissue formation

Polymer solutions with formulations GG and GGH were cooled to 45°C and mixed with the different cell pellets, chondrocytes (passage 1, 20×10^6 cells ml^{-1}), ACPCs (passage 4, 20×10^6 cells ml^{-1}), and MSCs (passage 4, 20×10^6 cells ml^{-1}). Cell-laden polymer solutions were pipetted into custom-made cylindrical Teflon molds (diameter 6 mm, height 2 mm) to be cross-linked with UV light (UV-Handleuchte lamp A., Hartenstein, Germany, wavelength: 365 nm, intensity at 3 cm: 1.2 mW cm^{-2} , irradiation time: 5 min). After cross-linking, hydrogel constructs were cultured for 1 or 28 days at 37°C and 5% CO_2 in chondrogenic differentiation medium consisting of high glucose DMEM (D6429, Sigma Aldrich) supplemented with 1% ITS + premix (BD Biosciences, Breda, The Netherlands), 0.1 μM dexamethasone (Sigma Aldrich), 0.2 mM L-ascorbic acid-2-phosphate (Sigma Aldrich), 10 ng ml^{-1} recombinant human TGF- β 1 (Peprotech), and 1% penicillin/streptomycin (final concentration: 100 units ml^{-1} penicillin and 100 $\mu\text{g ml}^{-1}$ streptomycin) to stimulate chondrogenesis of the embedded cells (37,38). Culture medium was refreshed twice a week and 0.1 μM monensin (Sigma Aldrich) was added to the culture medium of samples used for quantitative and histological evaluation, the night before sample harvest, to trap proteoglycan IV intracellularly(39).

Evaluation of (zone-specific) cartilage matrix production

Three samples ($n = 3$) of each hydrogel/cell type and donor combination were harvested at days 1 and 28. Half of each sample was weighed (wet weight), freeze dried, and weighed again (dry weight) to determine the water content. Next, samples were digested and GAG and DNA contents were measured with a dimethylmethylene blue (DMMB) assay and a QuantiT PicoGreen dsDNA kit, respectively, as previously described (16). Since the DMMB assay also detects the introduced HAMA, the GAG content measured at day 28 was corrected for the initial readout at day 1 for the cast samples containing a single cell type.

The other half of each sample was fixed overnight in 10% formalin, followed by dehydration through a graded ethanol series, and clearing in xylene. Sequentially, samples were embedded in paraffin, and tissue sections with a thickness of 5 μm were cut. Tissue sections were stained with safranin-O, fast green, and hematoxylin to visualize proteoglycans (red), collagens (green), and cell nuclei (purple), respectively (40). Collagen types I, II, and VI, and proteoglycan IV were visualized with immunohistochemistry as previously described (25,41). All sections were evaluated and photographed with a light microscope (Olympus BX51 microscope, Olympus DP70 camera, Hamburg, Germany).

Gene expression of embedded cells

At days 1 and 28, three samples ($n = 3$) of each condition were harvested in RLT-buffer (Qiagen, Germany). Samples were crushed manually and then minced with a QIAshredder column (Qiagen, Germany). Subsequently, mRNA was isolated, and amplification and cDNA synthesis were performed, all as previously described (34). Quantitative RT-PCR (qPCR) was used to analyze the mRNA expression levels of aggrecan (ACAN), collagen type II (COL2A1), collagen type I (COL1A1), proteoglycan IV (PRG4), collagen type X (COL10A1), and the housekeeping gene HPRT1 for normalization, using the primers as reported by Levato et al. (2017) (34).

Bioprinted two-zone constructs

Three-dimensional bioprinting of two-zone constructs

Two-zone constructs were bioprinted with an optimized bio-ink for each region. Based on the results of the previous experiments, the combination of

hydrogel formulation GGH with ACPCs was selected for the superficial region and the combination of formulation GGH with MSCs was selected for the middle/deep region. Cell-laden polymer solutions were prepared as described in section “2.5. Construct Preparation for the Screening of Zone-Specific Cartilage-Like Tissue Formation” ($N = 1$). Sequentially, the bio-inks were loaded into a 3DDiscovery bioprinter (RegenHU) and printed on top of each other in cuboid sheets (15 x 15 mm, 3 mm in height, of which 2 mm middle/deep region and 1 mm superficial region) with optimized print settings (Table S1). To reduce the shear stresses on the embedded cells, a 22-gauge conical needle (Precision Tip PN, Nordson EFD) was used, with a decreased print pressure compared to the settings used for the filament screening (Table S1). After printing, the printed sheet was covered with a glass slide and cross-linked for 96 s with a Bluepoint 4 UV lamp (point light source, wavelength range: 300–600 nm, UV-A intensity at 5 cm = 103 mW cm⁻², Hönle UV Technology AG, Gräfelfing, Germany). The printed sheets were cut into nine samples of (5 x 5 mm, 3 mm in height) which were cultured in chondrogenic differentiation medium as described in section “Construct Preparation for the Screening of Zone-Specific Cartilage-Like Tissue Formation.” As controls, constructs of the same dimensions consisting solely out of GGH with ACPCs or MSCs were printed and cross-linked. Additionally, both bio-inks were cast in cylindrical Teflon molds and constructs were cross-linked with the Bluepoint 4 UV lamp using the same protocol as for the printed constructs, to generate unprinted controls.

Evaluation of two-zone constructs

Samples of all conditions were harvested at days 1, 28, and 42 of culture to evaluate (zone-specific) cartilage-like tissue formation as described in section “Evaluation of (Zone-Specific) Cartilage Matrix Production.” For the evaluation of the gene expression of embedded cells, the upper part of the superficial region and bottom part of the middle/deep region of the two-zone constructs were separated to be analyzed individually. The other constructs were evaluated as a whole, all according to the protocol described in section “Gene Expression of Embedded Cells.”

Statistics

For the screening of (zone-specific) chondrogenesis (content and gene expression) in the bio-inks, differences between cell types within a hydrogel formulation

and time points were determined with a randomized block design ANOVA to correct for donor variability. Differences between the hydrogel formulations GG and GGH within a cell type were determined with an independent *t*-test. Comparison of the gene expression levels or GAG and DNA contents of the printed constructs (layered or single layer) were determined with a one-way ANOVA per time point. Furthermore, differences in content and gene expression levels between printed and cast constructs were determined with an independent *t*-test. Normality and homogeneity were assumed, and a significance level of $p < 0.025$ was used for all statistical tests (Bonferroni correction of the *p* value to correct for the double tests). When the ANOVA tests indicated a significant difference, a Bonferroni *post hoc* test was performed.

Results

Screening of filament stability

All filaments printed with 10% gelMA (formulation G) were able to bridge a gap of 2 mm before breaking, while only three out of five filaments could bridge a 4-mm gap (Figure 1). The addition of 0.5% gellan to the gelMA hydrogel (formulation GG) increased the bridging distance; 100% of the filaments were able to bridge a gap of 4 mm wide without breaking and one filament could also bridge a gap of 8 mm wide. The bridging distance was further increased by the addition of HAMA (formulation GGH). Printing with this formulation allowed the bridging of gaps of 8 mm wide for all filaments and one filament was able to bridge a gap of 16 mm.

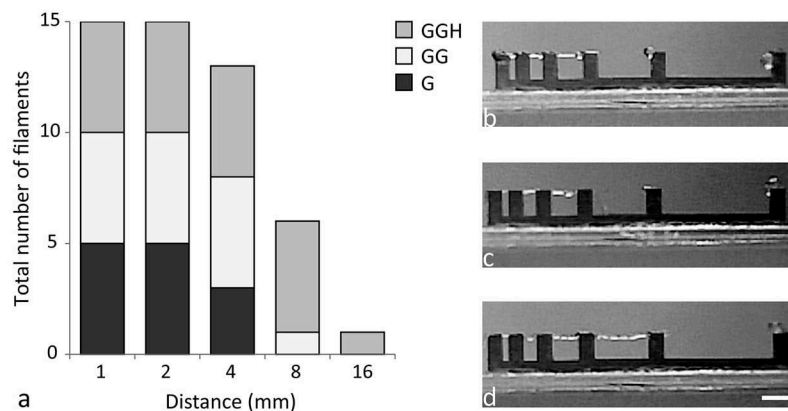


Figure 1 Evaluation of filament collapse in gap bridging as a measure of filament stability. Overview of the total number of filaments out of five that could bridge each distance (a). Each shade of gray represents the proportion of filaments for each separate hydrogel formulation. Three-dimensional printing with formulation GGH formed the most stable filaments as these could bridge the largest gaps without collapsing (8 mm, all evaluated filaments; 16 mm, one filament). Examples of the filament appearance of formulations G (b), GG (c), and GGH (d). Scale bar represents 4 mm for all pictures. With G = 10% gelMA, GG = 10% gelMA + 0.5% gellan gum, and GGH = 9.5% gelMA + 0.5% gellan gum + 0.5% HAMA.

Screening of (zone-specific) chondrogenesis in GG and GGH hydrogels

GAG content normalized to the DNA content was significantly lower in chondrocyte-laden hydrogels compared to ACPC-, and MSC-laden constructs at day 28 (Figure 2a). Moreover, no differences in GAG content were observed between the hydrogel formulations (GG and GGH) for each cell type. The DNA content normalized to the dry weight and the water content normalized to the wet weight were similar for all cell types and hydrogel formulations (Figure 2b,c). Additionally, no changes in DNA per dry weight and water per wet weight contents were observed between days 1 and 28 of culture.

MSC-laden hydrogels, and to a lesser extent ACPC-laden hydrogels, revealed intense staining for GAGs (safranin-O) and collagen type II (Figure 3a,b). In addition, large cell clusters formed in these hydrogels, and most intense staining was observed around these clusters. In contrast, hydrogels with embedded chondrocytes had limited areas that stained positive for GAGs and collagen type II and contained predominantly single cells. All hydrogel samples stained positive for collagen type I, both at day 1 and day 28 (Figure 3c). Furthermore, the staining intensity was higher at day 28 compared to their day 1 control. No clear differences in staining intensity for safranin-O, collagen type I, or collagen type II were observed between hydrogel formulations GG and GGH with the same cell type.

For all cell types, aggrecan and collagen type II mRNA expression relative to the housekeeping gene HPRT was upregulated at day 28 compared to day 1 (Figure 4a). No significant differences were observed

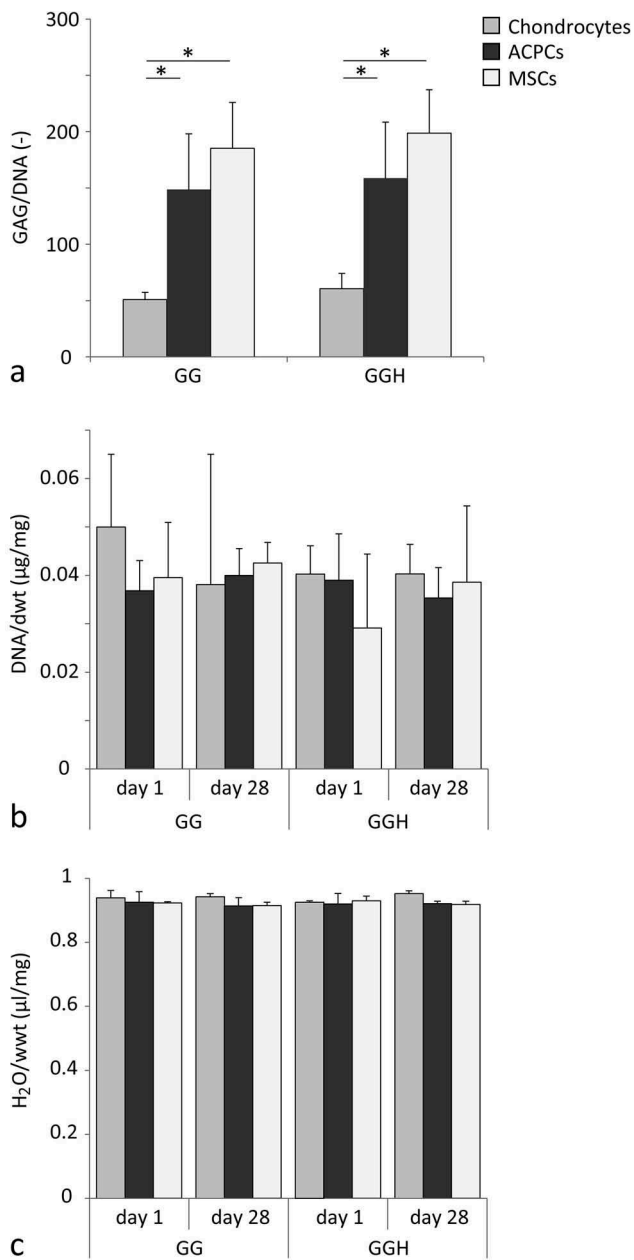


Figure 2 Quantitative evaluation of cartilage-like tissue formation of the three cell types in GG and GGH hydrogels ($N = 3$, $n = 3$). GAG/DNA was highest in samples with MSCs and ACPCs (a). No differences in DNA/dry weight (dwt, b) or water/wet weight (H_2O/wwt , c) were measured between cell types or hydrogel formulations. * Indicates a significant difference ($p < 0.025$). Values represent the mean \pm standard deviation. With GG = 10% gelMA + 0.5% gellan gum, and GGH = 9.5% gelMA + 0.5% gellan gum + 0.5% HAMA.

for aggrecan gene expression levels between the different cell types in formulation GG at day 28. However, in formulation GGH, chondrocytes had significantly lower aggrecan mRNA levels compared to ACPCs and MSCs at day 28. In addition, MSCs showed the highest mRNA expression levels of collagen type II at the end

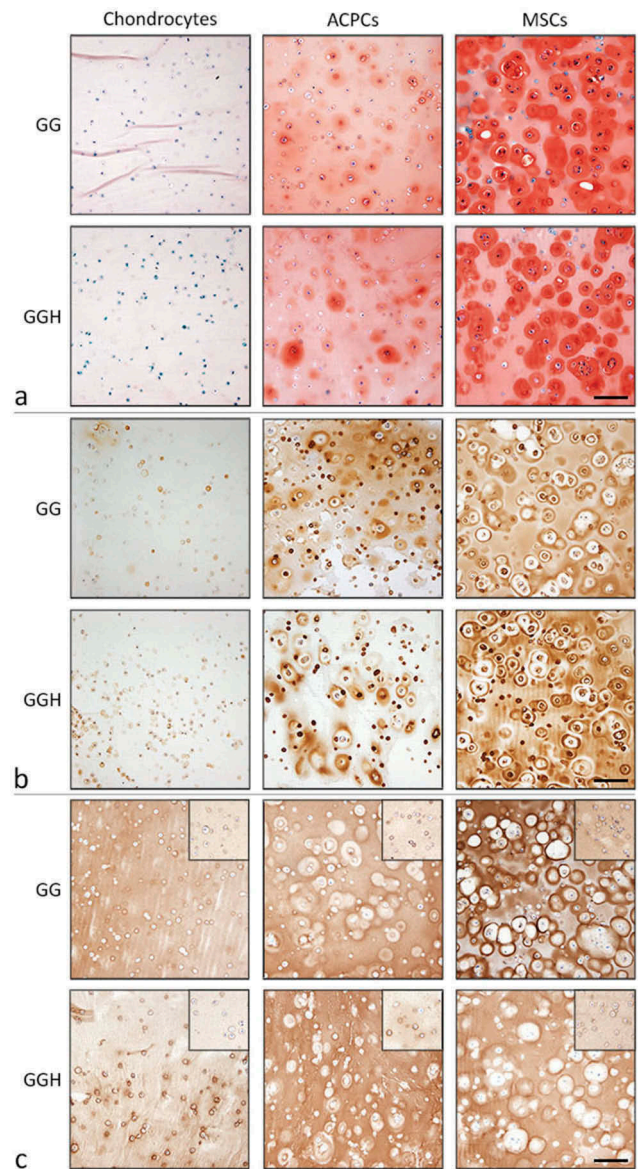


Figure 3 Histological assessment of cartilage-like tissue formation at day 28 in hydrogel constructs with the different cell types and formulations ($N = 3$, $n = 3$). Safranin-O/fast green staining (a). Collagen type II staining (b). Collagen type I staining with the day 1 appearance in the inserts (c). Scale bars represent 100 μm for all images. With GG = 10% gelMA + 0.5% gellan gum, and GGH = 9.5% gelMA + 0.5% gellan gum + 0.5% HAMA.

of the culture period (Figure 4b). Furthermore, collagen type I mRNA expression was highest for MSCs at day 1, but no differences were measured between the different cell types at day 28 when being cultured in hydrogel GGH (Figure 4c). Moreover, ACPCs embedded in formulation GG had significantly lower mRNA levels for collagen type I compared to chondrocytes and MSCs in this formulation at day 28. No significant differences in gene expression levels were observed between the

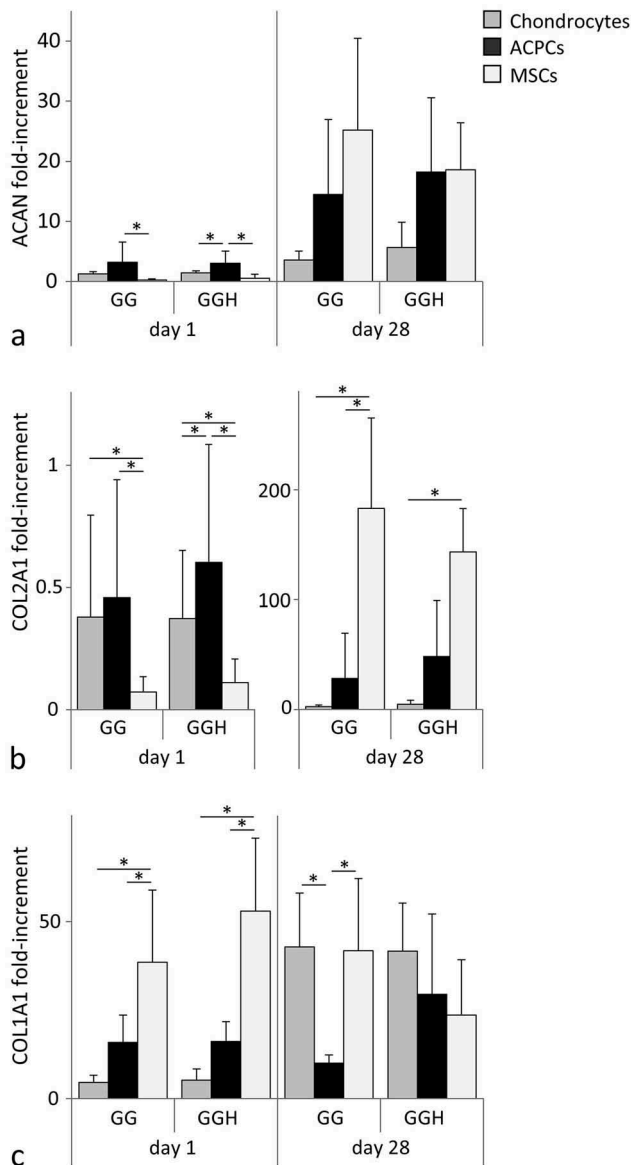


Figure 4 mRNA expression of chondrogenic genes relative to the housekeeping gene (HPRT), for chondrocytes, ACPCs, and MSCs, within the two hydrogel formulations (GG and GGH, $N = 3$, $n = 3$). After 28 days of culture, aggrecan (ACAN) expression of chondrocytes in hydrogel GG was lower compared to ACPCs and MSCs in this hydrogel formulation (a). Collagen type II (COL2A1) gene expression increased for all cell types with culture, but highest mRNA levels were measured in MSC-laden constructs at day 28, please note the different scale on the y-axes. (b). Collagen type I (COL1A1) expression was highest for MSCs at day 1, but at day 28 similar levels were measured for all cell types in formulation GGH, while a lower expression was observed for ACPCs in formulation GG (c). No significant differences were observed between formulation GG and GGH for any of the cell types. Values represent the mean \pm standard deviation. With G = 10% gelMA, GG = 10% gelMA + 0.5% gellan gum, and GGH = 9.5% gelMA + 0.5% gellan gum + 0.5% HAMA. * Indicates a significant difference ($p < 0.025$).

hydrogel formulations, GG and GGH, for each of the cell types.

All cell types synthesized proteoglycan IV at day 28 of culture, as determined with immunohistochemistry (Figure 5a and S1). No differences were observed between formulations GG and GGH for each cell type. Moreover, proteoglycan IV mRNA was detected for all cell types at both day 1 and day 28 (Figure 5b). Significantly higher proteoglycan IV mRNA expression levels were observed for chondrocytes and ACPCs embedded in GGH compared to MSCs in this formulation. In formulation GG, ACPCs contained significantly higher proteoglycan IV mRNA levels at day 28 compared to both chondrocytes and MSCs in this formulation at this time point. Furthermore, collagen type X mRNA expression was similar for all cell types at day 1 and 28, except for chondrocytes embedded in formulation GG at day 28, which had significantly lower collagen type X mRNA levels compared to MSCs.

Printed two-zone constructs

Constructs with two regions were successfully 3D printed with ACPC-laden GGH for the top region (representing the superficial zone cartilage) and MSC-laden GGH for the bottom region (representing the middle/deep zone cartilage), as well as constructs consisting of only one of the two material/cell combinations. GAG content normalized to the DNA content increased during culture for both the two-zone constructs and the single-zone constructs (Figure 6a). In addition, the DNA content normalized to the sample dry weight remained stable during culture for all constructs (Figure 6b). After 42 days of culture, the two regions of the two-zone constructs could be distinguished on histological sections. In both regions, cell clusters had formed, which stained positive for GAGs (safranin-O, Figure 6c). The extracellular matrix surrounding the cell clusters also stained positive for GAGs. Immunohistochemical stainings of collagen types I and II stained positive in both regions of the two-zone constructs (Figure 6d,e). Collagen type II staining was most intense in and around the cell clusters, while the collagen type I staining was weakest at these locations. Moreover, both the ACPCs in the superficial region and the MSCs in the middle/deep region stained positive for proteoglycan IV (Figure 6f).

No significant differences in mRNA expression of aggrecan were observed between conditions within each time point (Figure 7a). A significantly higher collagen

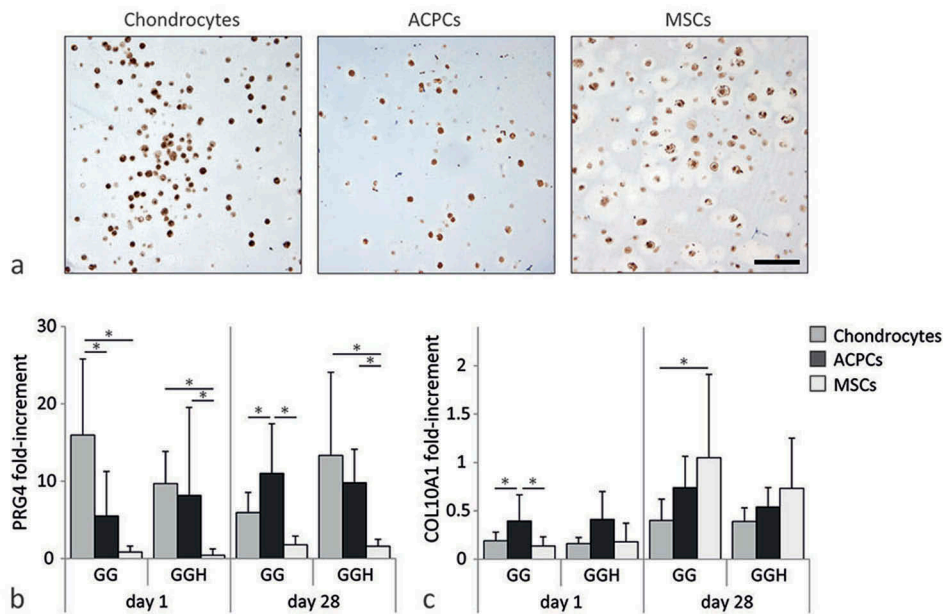


Figure 5 Evaluation of zone-specific cartilage production ($N = 3$, $n = 3$). All cell types produced proteoglycan IV (PRG4) in formulation GGH during culture (a). Highest relative mRNA expression of proteoglycan IV was measured in chondrocytes and ACPCs at day 28. Relative mRNA expression of collagen type X (COL10A1) was similar for all cell types after 28 days of culture (b). Scale bar represents 100 μm for all images. Values represent the mean \pm standard deviation. With GG = 10% gelMA + 0.5% gellan gum, and GGH = 9.5% gelMA + 0.5% gellan gum + 0.5% HAMA. * Indicates a significant difference ($p < 0.025$).

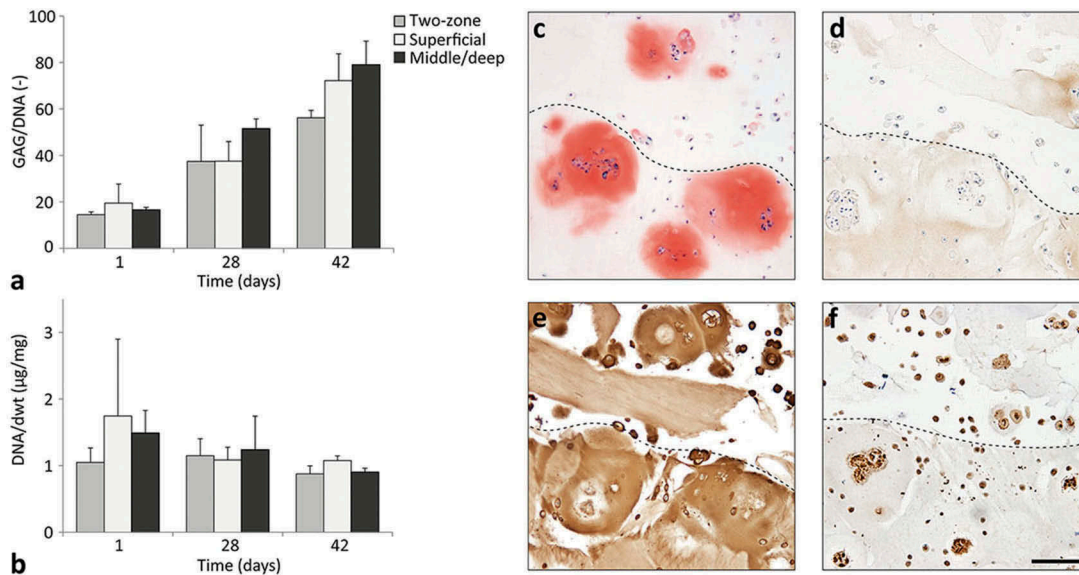


Figure 6 Cartilage production within the printed two-zone constructs ($N = 1$, $n = 3$). GAG normalized to the DNA content (a) and DNA normalized to the dry weight (dwt, b) for printed two-zone constructs (two-zone), printed superficial zone only constructs (superficial), and printed middle/deep zone constructs (middle/deep). Values represent the mean \pm standard deviation. Histological assessment of two-zone constructs for safranin-O (c), collagen type I (d), collagen type II (e), and proteoglycan IV (f). The dotted lines indicate the transition between the superficial zone (top) and middle/deep zone (bottom). Scale bar represents 100 μm for all images.

type II gene expression level was measured for the ACPCs in the superficial region of the two-zone constructs, compared to the ACPCs and MSCs in the single-zone constructs (Figure 7b). Furthermore, mRNA expression of collagen type I was similar in both regions of the two-zone

constructs, and in the single-zone controls at all time points (Figure 7c). In addition, no differences in proteoglycan IV gene expression were measured between the ACPCs in the superficial region or the MSCs in the middle/deep region of the two-zone constructs, nor in

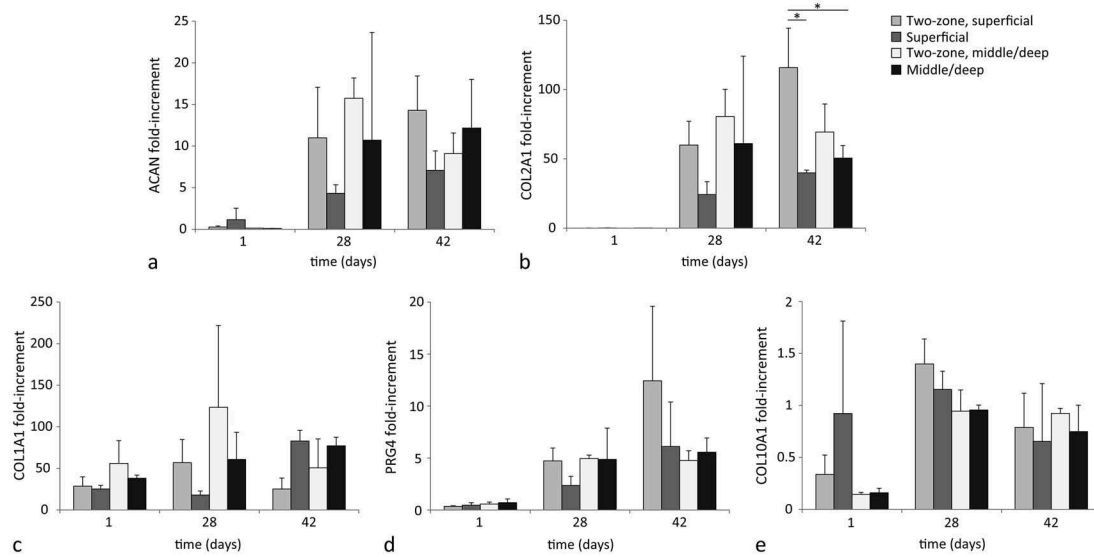


Figure 7 Gene expression for cells in the superficial and middle/deep region of the two-zone constructs (“two-zone, superficial” and “two-zone, middle/deep,” respectively), and the single-zone constructs (“superficial” or “middle/deep,” $N = 1$, $n = 3$). Expression levels of mRNA for aggrecan (ACAN, a), collagen type II (COL2A1, b), collagen type I (COL1A1, c), proteoglycan IV (PRG4, d), and collagen type X (COL10A1, e). * Indicates a significant difference ($p < 0.025$) and the values represent the mean \pm standard deviation.

the single-zone constructs (Figure 7d). Furthermore, mRNA expression of collagen type X was similar for all printed constructs at all time points (Figure 7e).

Along with the printed single-zone constructs, also cast controls were cultured. Histological assessment of the cast controls revealed more intense safranin-O staining compared to the printed single-zone hydrogels at day 42 (Figure 8a). Furthermore, all printed constructs contained several single cells without an intensely stained matrix surrounding them, while these single cells were only observed sporadically in the cast controls. Additionally, the histological appearance of the printed single-zone constructs was similar to the matching region in the printed two-zone constructs. The GAG content normalized to the DNA content, and the mRNA expression levels for aggrecan and collagen type II revealed a similar trend to that observed in the histological sections; lower values in printed hydrogels compared to the cast hydrogels (Figure 8b, 8c, and 8d). Furthermore, collagen type I staining was more intense and relative mRNA expression was significantly higher for the printed constructs compared to the cast controls with the same cell type (Figure 8a,e).

Discussion

The results of this study demonstrate improved shape-fidelity of printed gelMA/gellan filaments with the incorporation of HAMA (formulation GGH). Moreover, ACPCs, MSCs, and, to a lesser extent, chondrocytes produced cartilage-like tissue in cast GGH hydrogels. More specifically, MSCs expressed the

highest levels of collagen type II mRNA, while ACPCs exhibited higher proteoglycan IV mRNA expression levels compared to the MSCs. Therefore, two-zone constructs were printed with GGH bio-ink with ACPCs in the top region and MSCs in the middle/deep region. Although both the ACPCs and MSCs produced GAGs and collagen type II in their designated zone, bioprinting of both cell types resulted in changes in the quality of the produced neo-cartilage, compared to cast cell-laden hydrogel controls. Both the ACPCs and MSC-laden constructs stained less intense for GAGs after printing, while an increase in collagen type I staining intensity was observed, although collagen type II staining remained prominent. Similar trends were detected for mRNA expression levels and GAG content. These results strongly suggest that the printing procedure influenced the chondrogenesis of the embedded cells. Comparable observations were made by Müller et al. (2016) (42), who demonstrated that high shear stresses due to relatively small nozzle diameters delayed matrix synthesis and affected cell spreading, but not cell viability. They reported compromised chondrocyte behavior when exposing the cells to shear forces of above ~ 160 Pa. Furthermore, finite-element simulations estimated that shear forces larger than 160 Pa can already occur when printing cell-laden alginate-based hydrogels with a pressure of 6 kPa and the needle geometry used in the current paper. Due to the relatively high yield stress of gelMA/gellan/HAMA hydrogels, we used a significantly higher pressure (80 kPa) for successful filament deposition. Therefore, the

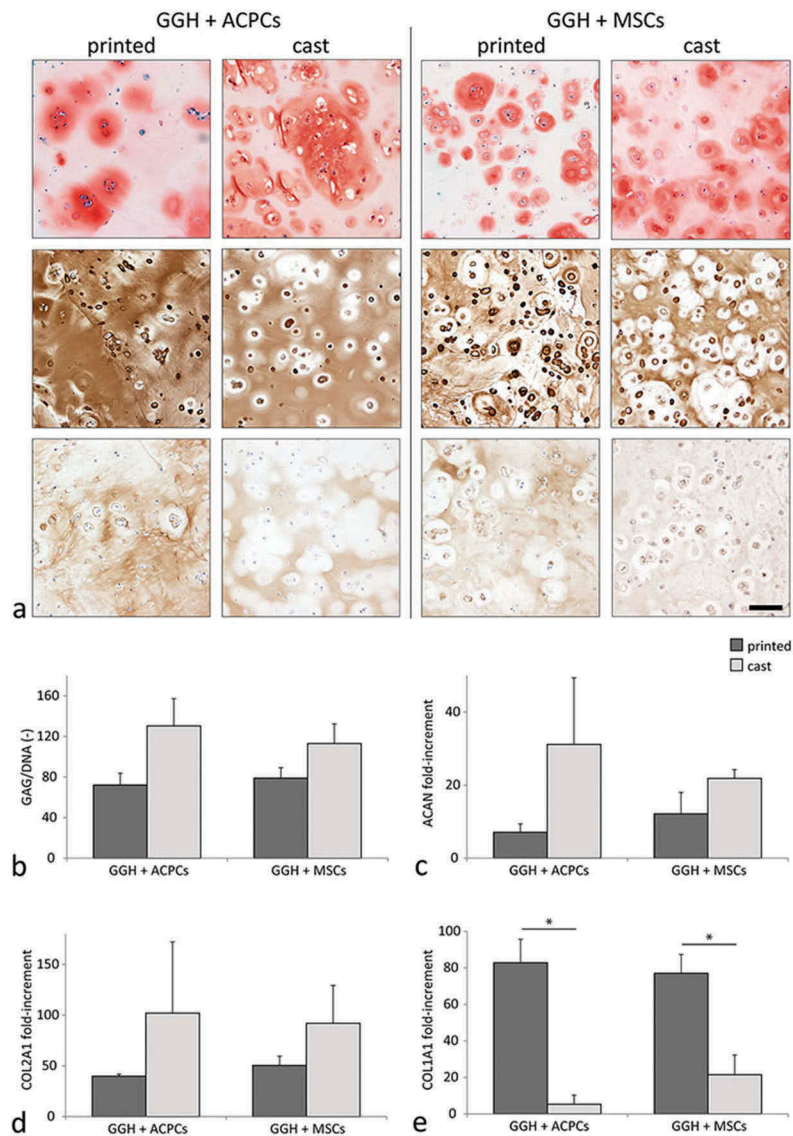


Figure 8 Chondrogenic potential of ACPCs and MSCs in printed and cast hydrogels at day 42 of culture in GG or GGH hydrogels ($N = 1$, $n = 3$). Histological assessment of GAGs (safranin-O, top), collagen type II (middle), and collagen type I (bottom) matrix production; scale bar indicates 100 μm for all images (a). GAG content normalized to the DNA content for printed and cast hydrogels with ACPCs or MSCs (b). Relative gene expression of aggrecan (ACAN, c), collagen type 2 (COL2A1, d), and collagen type I (COL1A1, e) for printed and cast hydrogels with ACPCs or MSCs. Values represent the mean \pm standard deviation. With GG = 10% gelMA + 0.5% gellan gum, and GGH = 9.5% gelMA + 0.5% gellan gum + 0.5% HAMA. * Indicates a significant difference ($p < 0.025$).

embedded ACPCs and MSCs were likely exposed to high shear forces, larger than 160 Pa during printing, which could explain the differences in matrix deposition observed between printed and cast constructs. These findings underscore that printing processes can influence other biological functions of embedded cells than just the viability, while often only the viability is checked to confirm successful printing of cells (43–45). Therefore, we believe that more extensive biological evaluations after printing, as well as the inclusion of cast control samples, are essential for future evaluation of bio-inks. Such more extensive assessments will

provide valuable insights in the boundary conditions for effective bioprinting (42).

Although the detailed mechanism behind the longer term influence of the printing process on the cells is currently unclear, it is known that shear forces can deform cells, causing cell adaptation and realignment of the cytoskeleton (43,46). Such adaptations start already after several seconds of mechanical stress, and might therefore play a role in the altered cell behavior observed after printing. Moreover, cell deformations were also demonstrated to steer MSC differentiation fate (47,48). For example, stretching of MSCs stimulates differentiation

toward the myogenic lineage (47) and shear forces via fluid flow can drive MSC differentiation into the osteogenic lineage (48). Thus, gaining deeper understanding of these processes might provide printing protocols to steer cell fate in the future.

In the current study, also the possibility to improve the printability of a gelMA/gellan bio-ink with the incorporation of HAMA was explored. Indeed, the addition of HAMA increased the filament stability. On average, filaments printed with the bio-ink GG started to collapse when bridging a gap of 8 mm, while all evaluated filaments printed with bio-ink GGH were able to bridge this distance. This observation is in line with previous findings that demonstrated enhanced filament shape-fidelity, via an increase in viscosity and yield stress, by the incorporation of HAMA in gelMA or PEG-based hydrogels (22,24).

The incorporation of HAMA in a hydrogel has also been demonstrated to improve cartilage-like tissue formation by embedded chondrocytes (25). However, no significant differences in matrix production or gene expression by chondrocytes, ACPCs, or MSCs were observed due to the presence of HAMA in the current study (formulation GG compared to GGH). The effect of HAMA on chondrogenesis is expected to be the result of cell receptor binding with HAMA (i.e. CD44 and hyaluronan mediated motility receptor) (49–52). Chondrocytes, ACPCs, and MSCs all have membrane receptors capable of binding with HAMA and thus can be influenced by its presence (51,53). However, the effect of HAMA on chondrocytes embedded in PEG-based hydrogels was demonstrated to be dose-dependent (25), possibly via a negative feedback on chondrogenesis due to cell receptor binding with HAMA (31,37,51,54). Likely, the optimal HAMA concentration (0.5%), which was found for chondrocyte-laden gelMA and PEG-based hydrogels in previous studies, is dependent on the hydrogel platform itself and the type of cells (17,25). Although the presence of HAMA could not increase cartilage-like tissue formation or gene expression, it did improve filament stability. Therefore, gelMA/gellan/HAMA hydrogels were used for the fabrication of the two-zone constructs.

Significantly more cartilage matrix was produced by the ACPCs and MSCs compared to the chondrocytes. The GAG content measured in the chondrocyte-laden GG(H) hydrogels in the current study is in line with previously reported values for chondrocytes embedded in similar hydrogels (16,34). To obtain a sufficient amount of chondrocytes, the cells were expanded in monolayer culture, which is known to cause dedifferentiation (26). This may explain our findings, even though the growth factor TGF- β 1 was used to induce

redifferentiation. Alternatively, this observation may imply that the ACPCs and MSCs are more effective than chondrocytes for *in vitro* cartilage tissue-engineering when using GG(H) hydrogels. Furthermore, both ACPCs and MSCs can be expanded in monolayer culture to obtain large numbers of cells without losing their phenotype. For these reasons, ACPCs and MSCs may represent promising cell sources for cartilage tissue-engineering purposes. However, isolation of autologous ACPCs from a patient is associated with donor-site morbidity (55). Therefore, careful consideration of the harvest location is required or the use of allogeneic ACPCs should be explored (56). In contrast to ACPCs, autologous MSCs can be obtained from more accessible tissues compared to articular cartilage. However, a downside of MSCs for cartilage repair is their tendency to progress into hypertrophic chondrogenesis or to initiate endochondral bone formation after *in vivo* implantation (57). Strategies to overcome this may be the incorporation of growth factors, e.g. TGF- β , into the hydrogel to steer chondrogenic differentiation (30,58), or direct coculture of MSCs with, e.g. chondrocytes (59). However, further research on such methods is required for clinical translation of tissue-engineered cartilage constructs containing MSCs.

Based on the results from the cast hydrogel cultures, ACPCs were found most suitable for the fabrication of superficial zone cartilage, while MSCs have potential for the fabrication of middle and deep zone cartilage. The mRNA expression levels of proteoglycan IV were significantly higher in ACPCs compared to the MSCs in formulation GGH. As ACPCs are mainly found in the native superficial cartilage (28), it is likely that they retain their ability for producing superficial zone matrix components. Indeed, previous studies have also reported higher proteoglycan IV gene expression levels in ACPCs compared to MSCs (34,60). Furthermore, MSC-laden hydrogels stained more intensely for GAGs (safranin-O) and collagen type II compared to the chondrocyte or ACPC-laden hydrogels. Additionally, similar trends in gene expression levels were observed between these cell types at day 28. Therefore, MSCs may be beneficial for relatively fast production of hyaline-like cartilage within GGH constructs. Thus, MSCs in a GGH bio-ink form a promising combination for the fabrication of the middle and deep cartilage regions.

Two-zone constructs were successfully printed with different cell types in each zone. However, limited differences between the two regions were observed during culture (days 28 and 42), despite the differences observed in monocultures. MSCs produced slightly more GAGs compared to the ACPCs in the top layer, as observed with the safranin-O staining. However, GAG content

and aggrecan mRNA expression was similar for both layers at all time points. Furthermore, proteoglycan IV mRNA expression levels increased during the first 28 days of culture for both ACPCs and MSCs, reaching similar levels at days 28 and 42. This is in contrast to the proteoglycan IV mRNA expression levels measured for the cast hydrogels used for the evaluation of (zone-specific) cartilage-matrix production, where proteoglycan IV mRNA expression levels of MSCs did not increase during culture (mRNA expression relative to HPRT in the cast MSC-laden hydrogels of the zone-specific chondrogenesis screening: 0.6 ± 0.9 , in printed two-zone constructs: 5.0 ± 0.3 , and in printed single-zone constructs: 4.9 ± 3.0 , at day 28). This observation may indicate that the printing of MSCs stimulates gene expression of proteoglycan IV. Other studies demonstrated an increase in proteoglycan IV production by chondrocytes due to shear forces (6,60). However, a similar effect would then be expected for the ACPCs, which was not the case (mRNA expression relative to HPRT in the cast ACPC-laden hydrogels of the first experiment: 9.8 ± 4.0 , in printed two-zone constructs: 4.7 ± 1.2 , and in printed single-zone constructs: 2.4 ± 0.9 , at day 28). Possibly, ACPCs and MSCs react differently to the printing procedure, highlighting the importance of gaining deeper understanding of the effects of this process on cell behavior.

Although two-zone cartilage constructs were printed, limited zonal differences were observed after culture. Additional strategies to stimulate zone-specific matrix production by the embedded cells may improve zonal cartilage formation within hydrogel constructs. For example, the incorporation of biological cues, *e.g.* chondroitin sulfate, matrix metalloproteinase-sensitive peptides, growth factors, or differences in cell densities (12,61–63), all have been demonstrated to steer cells into producing zone-specific cartilage-like tissue. Furthermore, imposing mechanical loading (compression and shear) onto cell-laden hydrogel constructs was shown to increase cartilage-like matrix production (64,65), proteoglycan IV production at the hydrogel surface (6,66), and may it induce the characteristic alignment of collagen fibers (67,68).

Conclusions

GelMA/gellan/HAMA (GGH) hydrogel is a promising bio-ink that allows the printing of stable cell-laden hydrogel filaments. Cast GGH constructs supported chondrogenic differentiation of embedded ACPCs, MSCs, and, to a lesser extent, chondrocytes. However, cell differentiation was influenced by the printing procedure. The results of this study highlight the

importance of including cast controls when evaluating bioprinted cartilage constructs. Additionally, further evaluation of the influence of the printing process on advanced biological functions of embedded cells is required to provide more detailed boundary conditions for successful bioprinting.

Acknowledgments

The authors would like to thank J. Rudman for his help with the cell cultures, M. H. P. van Rijen for his help with the histology, and A. Abbadessa for the synthesis of HAMA. The primary antibody against collagen type II (II-II6B3) and collagen type VI (5C6), developed by T. F. Linsenmayer and E. S. Engvall, respectively, were obtained from the DSHB, developed under the auspices of the NICHD and maintained by The University of Iowa, Department of Biology, Iowa City, IA 52242.

Disclosure statement

No potential conflict of interest was reported by the authors.

Funding

The research leading to these results has received funding from the European Community's Seventh Framework Programme (FP7/2007-2013) under grant agreement n° 309962 (HydroZONES), the European Research Council under grant agreement 647426 (3D-JOINT), and the Dutch Arthritis Foundation (LLP-12).

References

1. Prakash D, Learmonth D. Natural progression of osteo-chondral defect in the femoral condyle. *Knee*. 2002;9(1):7–10. doi:10.1016/S0968-0160(01)00133-8.
2. Browne JE, Branch TP. Surgical alternatives for treatment of articular cartilage lesions. *J Am Acad Orthop Surg*. 2000;8(3):180–189.
3. Almarza AJ, Athanasiou KA. Design characteristics for the tissue engineering of cartilaginous tissues. *Ann Biomed Eng*. 2004;32(1):2–17.
4. Buckley MR, Gleghorn JP, Bonassar LJ, Cohen I. Mapping the depth dependence of shear properties in articular cartilage. *J Biomech*. 2008;41(11):2430–2437. doi:10.1016/j.jbiomech.2008.05.021.
5. Schuurman W, Klein TJ, Dhert WJA, van Weeren PR, Huttmacher DW, Malda J. Cartilage regeneration using zonal chondrocyte subpopulations: a promising approach or an overcomplicated strategy? *J Tissue Eng Regen Med*. 2015;9(6):669–678. doi:10.1002/term.1638.
6. Li Z, Yao S, Alini M, Grad S. Different response of articular chondrocyte subpopulations to surface motion. *Osteoarthritis and Cartilage*. 2007;15(9):1034–1041. doi:10.1016/j.joca.2007.03.001.

7. Hayes AJ, Hall A, Brown L, Tubo R, Caterson B. Macromolecular organization and in vitro growth characteristics of scaffold-free neocartilage grafts. *J Histochem Cytochem.* 2007;55(8):853–866. doi:10.1369/jhc.7A7210.2007.
8. Malda J, Ten Hoop W, Schuurman W, van Osch GJVM, van Weeren PR, Dhert WJA. Localization of the potential zonal marker clusterin in native cartilage and in tissue-engineered constructs. *Tissue Eng Part A.* 2010;16(3):897–904. doi:10.1089/ten.tea.2009.0376.
9. DiCesare PE, Mörgelein M, Carlson CS, Pasumarti S, Paulsson M. Cartilage oligomeric matrix protein: isolation and characterization from human articular cartilage. *J Orthopaedic Res.* 1995;13(3):422–428. doi:10.1002/jor.1100130316.
10. Brittberg M. Cell carriers as the next generation of cell therapy for cartilage repair: a review of the matrix-induced autologous chondrocyte implantation procedure. *Am J Sports Med.* 2010;38(6):1259–1271. doi:10.1177/0363546509346395.
11. Dewan AK, Gibson MA, Elisseff JH, Trice ME. Evolution of autologous chondrocyte repair and comparison to other cartilage repair techniques. *Biomed Res Int.* 2014;2014(Table 1):1–11. doi:10.1155/2014/272481.
12. Klein TJ, Malda J, Sah RL, Hutmacher DW. Tissue engineering of articular cartilage with biomimetic zones. *Tissue Eng Part B: Rev.* 2009;15(2):143–157. doi:10.1089/ten.teb.2008.0563.
13. Hollander AP, Dickinson SC, Kafienah W. Stem cells and cartilage development: complexities of a simple tissue. *Stem Cells.* 2010;28(11):1992–1996. doi:10.1002/stem.534.
14. Mouser VHM, Levato R, Bonassar LJ, DLima DD, Grande DA, Klein TJ, Saris DBF, Zenobi-Wong M, Gawlitta D, Malda J. Three-dimensional bioprinting and its potential in the field of articular cartilage regeneration. *Cartilage.* 2016 Sep 1. doi:10.1177/1947603516665445.
15. Malda J, Visser J, Melchels FP, Jüngst T, Hennink WE, Dhert WJA, Groll J, Hutmacher DW. 25th anniversary article: engineering hydrogels for biofabrication. *Adv Mater.* 2013 [cited 2014 Jul 10];25(36):5011–5028. <http://www.ncbi.nlm.nih.gov/pubmed/24038336>.
16. Mouser VHM, Melchels FPW, Visser J, Dhert WJA, Gawlitta D, Malda J. Yield stress determines bioprintability of hydrogels based on gelatin-methacryloyl and gellan gum for cartilage bioprinting. *Biofabrication.* 2016;8(3):035003. doi:10.1088/1758-5090/8/3/035003.
17. Levett PA, Melchels FPW, Schrobback K, Hutmacher DW, Malda J, Klein TJ. A biomimetic extracellular matrix for cartilage tissue engineering centered on photocurable gelatin, hyaluronic acid and chondroitin sulfate. *Acta Biomater.* 2014;10(1):214–223. doi:10.1016/j.actbio.2013.10.005.
18. Yue K, Trujillo-de Santiago G, Alvarez MM, Tamayol A, Annabi N, Khademhosseini A. Synthesis, properties, and biomedical applications of gelatin methacryloyl (GelMA) hydrogels. *Biomaterials.* 2015;73:254–271. doi:10.1016/j.biomaterials.2015.08.045.
19. Gao G, Schilling AF, Hubbell K, Yonezawa T, Truong D, Hong Y, Dai G, Cui X. Improved properties of bone and cartilage tissue from 3D inkjet-bioprinted human mesenchymal stem cells by simultaneous deposition and photocrosslinking in PEG-GelMA. *Biotechnol Lett.* 2015;37(11):2349–2355. doi:10.1007/s10529-015-1921-2.
20. Billiet T, Gevaert E, De Schryver T, Cornelissen M, Dubrue P. The 3D printing of gelatin methacrylamide cell-laden tissue-engineered constructs with high cell viability. *Biomaterials.* 2014 [cited 2014 Aug 13];35(1):49–62. <http://www.ncbi.nlm.nih.gov/pubmed/24112804>.
21. Melchels FPW, Dhert WJA, Hutmacher DW, Malda J. Development and characterisation of a new bioink for additive tissue manufacturing. *J Mater Chem B.* 2014 [cited 2014 Aug 22];2(16):2282–2289. <http://xlink.rsc.org/?DOI=c3tb21280g>.
22. Schuurman W, Levett PA, Pot MW, van Weeren PR, Dhert WJA, Hutmacher DW, Melchels FPW, Klein TJ, Malda J. Gelatin-methacrylamide hydrogels as potential biomaterials for fabrication of tissue-engineered cartilage constructs. *Macromol Biosci.* 2013 [cited 2014 Sep 9];13(5):551–561. <http://www.ncbi.nlm.nih.gov/pubmed/23420700>.
23. Levett PA, Hutmacher DW, Malda J, Klein TJ. Hyaluronic acid enhances the mechanical properties of tissue-engineered cartilage constructs. *PLoS ONE.* 2014 [cited 2014 Dec 3];9(12):e113216. <http://www.ncbi.nlm.nih.gov/pubmed/25438040>.
24. Abbadessa A, Landín M, Oude Blenke E, Hennink WE, Vermonden T. Two-component thermosensitive hydrogels: phase separation affecting rheological behavior. *Eur Polym J.* 2017;92(December2016):13–26. doi:10.1016/j.eurpolymj.2017.04.029.
25. Mouser VHM, Abbadessa A, Levato R, Hennink WE, Vermonden T, Gawlitta D, Malda J. Development of a thermosensitive HAMA-containing bio-ink for the fabrication of composite cartilage repair constructs. *Biofabrication.* 2017;9(1):015026. doi:10.1088/1758-5090/aa6265.
26. Ma B, Leijten JCH, Wu L, Kip M, van Blitterswijk CA, Post JN, Karperien M. Gene expression profiling of dedifferentiated human articular chondrocytes in monolayer culture. *Osteoarthritis and Cartilage.* 2013;21(4):599–603. doi:10.1016/j.joca.2013.01.014.
27. Jiang Y, Tuan RS. Origin and function of cartilage stem/progenitor cells in osteoarthritis. *Nat Rev Rheumatol.* 2015;11(4):206–212. doi:10.1038/nrrheum.2014.200.
28. Dowthwaite GP. The surface of articular cartilage contains a progenitor cell population. *J Cell Sci.* 2004;117(6):889–897. doi:10.1242/jcs.00912.
29. Dominici M, Le Blanc K, Mueller I, Slaper-Cortenbach I, Marini F, Krause D, Deans R, Keating A, Prockop D, Horwitz E. Minimal criteria for defining multipotent mesenchymal stromal cells. The international society for cellular therapy position statement. *Cytotherapy.* 2006 [cited 2014 Jul 9];8(4):315–317. <http://www.ncbi.nlm.nih.gov/pubmed/16923606>.
30. Spiller KL, Maher SA, Lowman AM. Hydrogels for the repair of articular cartilage defects. *Tissue Eng Part B: Rev.* 2011;17(4):281–299. doi:10.1089/ten.teb.2011.0077.
31. Hachet E, Van Den Berghe H, Bayma E, Block MR, Auzély-Velty R. Design of biomimetic cell-interactive substrates using hyaluronic acid hydrogels with tunable

- mechanical properties. *Biomacromolecules*. 2012;13(6):1818–1827. doi:10.1021/bm300324m.
32. Ribeiro A, Blokzijl MM, Levato R, Visser CW, Castilho M, Hennink WE, Vermonden T, Malda J. Assessing bioink shape fidelity to aid material development in 3D bioprinting. *Biofabrication*. 2017 Oct 4;10:014102. doi:10.1088/1758-5090/aa90e2.
 33. Williams R, Khan IM, Richardson K, Nelson L, McCarthy HE, Analbelsi T, Singhrao SK, Dowthwaite GP, Jones RE, Baird DM, et al. Identification and clonal characterisation of a progenitor cell sub-population in normal human articular cartilage Agarwal S, editor. *PLoS ONE*. 2010;5(10):e13246. doi:10.1371/journal.pone.0013246.
 34. Levato R, Webb WR, Otto IA, Mensinga A, Zhang Y, van Rijen M, van Weeren R, Khan IM, Malda J. The bio in the ink: cartilage regeneration with bioprintable hydrogels and articular cartilage-derived progenitor cells. *Acta Biomater*. 2017 Aug;61:41–53. doi:10.1016/j.actbio.2017.08.005.
 35. Pittenger MF. Multilineage potential of adult human mesenchymal stem cells. *Science*. 1999;284(5411):143–147. doi:10.1126/science.284.5411.143.
 36. Benders KEM, Boot W, Cokelaere SM, Van Weeren PR, Gawlitta D, Bergman HJ, Saris DBF, Dhert WJA, Malda J. Multipotent stromal cells outperform chondrocytes on cartilage-derived matrix scaffolds. *Cartilage*. 2014;5(4):221–230. doi:10.1177/1947603514535245.
 37. Benya P. Dedifferentiated chondrocytes reexpress the differentiated collagen phenotype when cultured in agarose gels. *Cell*. 1982;30(1):215–224. doi:10.1016/0092-8674(82)90027-7.
 38. Guo J, Jourdain GW, MacCallum DK. Culture and growth characteristics of chondrocytes encapsulated in alginate beads. *Connect Tissue Res*. 1989;19(2–4):277–297. doi:10.3109/03008208909043901.
 39. Schumacher BL, Hughes CE, Kuettner KE, Caterson B, Aydelotte MB. Immunodetection and partial cDNA sequence of the proteoglycan, superficial zone protein, synthesized by cells lining synovial joints. *J Orthopaedic Res*. 1999;17(1):110–120. doi:10.1002/jor.1100170117.
 40. Wall A, Board T. Chemical basis for the histological use of safranin O in the study of articular cartilage. In: Banaszkiwicz PA, Kader DF, editors. *Classic papers in orthopaedics*. Vol. 53. London: Springer London; 2014. p. 433–435. doi:10.1007/978-1-4471-5451-8_110.
 41. Abbadessa A, Mouser VHM, Blokzijl MM, Gawlitta D, Dhert WJA, Hennink WE, Malda J, Vermonden T. A synthetic thermosensitive hydrogel for cartilage bioprinting and its biofunctionalization with polysaccharides. *Biomacromolecules*. 2016;17(6):2137–2147. doi:10.1021/acs.biomac.6b00366.
 42. Müller M, Öztürk E, Arlov Ø, Gatenholm P, Zenobi-Wong M. Alginate sulfate–nanocellulose bioinks for cartilage bioprinting applications. *Ann Biomed Eng*. 2017;45(1):210–223. doi:10.1007/s10439-016-1704-5.
 43. Ersumo N, Witherel CE, Spiller KL. Differences in time-dependent mechanical properties between extruded and molded hydrogels. *Biofabrication*. 2016;8(3):035012. doi:10.1088/1758-5090/8/3/035012.
 44. Chang R, Nam J, Sun W. Effects of dispensing pressure and nozzle diameter on cell survival from solid freeform fabrication-based direct cell writing. *Tissue Eng Part A*. 2008;14(1):41–48. doi:10.1089/ten.a.2007.0004.
 45. Nair K, Gandhi M, Khalil S, Yan KC, Marcolongo M, Barbee K, Sun W. Characterization of cell viability during bioprinting processes. *Biotechnol J*. 2009;4(8):1168–1177. doi:10.1002/biot.200900004.
 46. Matthews BD. Cellular adaptation to mechanical stress: role of integrins, Rho, cytoskeletal tension and mechanosensitive ion channels. *J Cell Sci*. 2006;119(3):508–518. doi:10.1242/jcs.02760.
 47. Yang Y, Beqaj S, Kemp P, Ariel I, Schuger L. Stretch-induced alternative splicing of serum response factor promotes bronchial myogenesis and is defective in lung hypoplasia. *J Clin Invest*. 2000;106(11):1321–1330. doi:10.1172/JCI8893.
 48. Sonam S, Sathe SR, Yim EKF, Sheetz MP, Lim CT. Cell contractility arising from topography and shear flow determines human mesenchymal stem cell fate. *Sci Rep*. 2016;6(October2015):20415. doi:10.1038/srep20415.
 49. Yasuda T. Nuclear factor- κ B activation by type II collagen peptide in articular chondrocytes: its inhibition by hyaluronan via the receptors. *Modern Rheumatology*. 2012;23(6):1116–1123. doi:10.1007/s10165-012-0804-9.
 50. Viola M, Vignetti D, Karousou E, D'Angelo ML, Caon I, Moretto P, De Luca G, Passi A. Biology and biotechnology of hyaluronan. *Glycoconj J*. 2015;32(3–4):93–103. doi:10.1007/s10719-015-9586-6.
 51. Akmal M, Singh A, Anand A, Kesani A, Aslam N, Goodship A, Bentley G. The effects of hyaluronic acid on articular chondrocytes. *J Bone Joint Surg - Br Volume*. 2005 [cited 2014 Aug 27];87-B(8):1143–1149. <http://www.ncbi.nlm.nih.gov/pubmed/16049255>.
 52. Ariyoshi W, Takahashi N, Hida D, Knudson CB, Knudson W. Mechanisms involved in enhancement of the expression and function of aggrecanases by hyaluronan oligosaccharides. *Arthritis Rheum*. 2012;64(1):187–197. doi:10.1002/art.33329.
 53. Bian L, Guvendiren M, Mauck RL, Burdick JA. Hydrogels that mimic developmentally relevant matrix and N-cadherin interactions enhance MSC chondrogenesis. *Proc Natl Acad Sci*. 2013;110(25):10117–10122. doi:10.1073/pnas.1214100110.
 54. Schuh E, Hofmann S, Stok K, Notbohm H, Müller R, Rotter N. Chondrocyte redifferentiation in 3D: the effect of adhesion site density and substrate elasticity. *J Biomed Mater Res Part A*. 2012 [cited 2014 Nov 20];100(1):38–47. <http://www.ncbi.nlm.nih.gov/pubmed/21972220>.
 55. McCarthy HS, Richardson JB, Parker JCE, Roberts S. Evaluating joint morbidity after chondral harvest for Autologous Chondrocyte Implantation (ACI): a study of ACI-treated ankles and hips with a knee chondral harvest. *Cartilage*. 2016;7(1):7–15. doi:10.1177/1947603515607963.

56. Matricali GA, Dereymaeker GPE, Luvten FP. Donor site morbidity after articular cartilage repair procedures: a review. *Acta Orthop Belg.* 2010;76(5):669–674.
57. Visser J, Gawlitta D, Benders KEM, Toma SMH, Pouran B, van Weeren PR, Dhert WJA, Malda J. Endochondral bone formation in gelatin methacrylamide hydrogel with embedded cartilage-derived matrix particles. *Biomaterials.* 2015 [cited 2014 Oct 24];37:174–182. <http://linkinghub.elsevier.com/retrieve/pii/S0142961214010679>.
58. Jung HH, Park K, Han DK. Preparation of TGF- β 1-conjugated biodegradable pluronic F127 hydrogel and its application with adipose-derived stem cells. *J Controlled Release.* 2010;147(1):84–91. doi:10.1016/j.jconrel.2010.06.020.
59. De Windt TS, Saris DBF, Slaper-Cortenbach ICM, Van Rijen MHP, Gawlitta D, Creemers LB, De Weger RA, Dhert WJA, Vonk LA. Direct cell–cell contact with chondrocytes is a key mechanism in multipotent mesenchymal. *Tissue Eng Part A.* 2015;21(19–20):2536–2547. doi:10.1089/ten.tea.2014.0673.
60. Seol D, McCabe DJ, Choe H, Zheng H, Yu Y, Jang K, Walter MW, Lehman AD, Ding L, Buckwalter JA, et al. Chondrogenic progenitor cells respond to cartilage injury. *Arthritis Rheum.* 2012;64(11):3626–3637. doi:10.1002/art.34613.
61. Karimi T, Barati D, Karaman O, Moeinzadeh S, Jabbari E. A developmentally inspired combined mechanical and biochemical signaling approach on zonal lineage commitment of mesenchymal stem cells in articular cartilage regeneration. *Integr Biol.* 2015;7(1):112–127. doi:10.1039/C4IB00197D.
62. Tatman PD, Gerull W, Sweeney-Easter S, Davis JI, Gee AO, Kim D-H, Gee AO. Multiscale biofabrication of articular cartilage: bioinspired and biomimetic approaches. *Tissue Eng Part B: Rev.* 2015;21(6):543–559. doi:10.1089/ten.teb.2015.0142.
63. Trappmann B, Gautrot JE, Connelly JT, Strange DGT, Li Y, Oyen ML, Cohen Stuart MA, Boehm H, Li B, Vogel V, et al. Extracellular-matrix tethering regulates stem-cell fate. *Nat Mater.* 2012;11(8):742. doi:10.1038/nmat3387.
64. Wong M, Carter DR. Articular cartilage functional histomorphology and mechanobiology: a research perspective. *Bone.* 2003;33(1):1–13. doi:10.1016/S8756-3282(03)00083-8.
65. Klein TJ, Rizzi SC, Reichert JC, Georgi N, Malda J, Schuurman W, Crawford RW, Huttmacher DW. Strategies for zonal cartilage repair using hydrogels. *Macromol Biosci.* 2009;9(11):1049–1058. doi:10.1002/mabi.200900176.
66. Grad S, Lee CR, Gorna K, Gogolewski S, Wimmer MA, Alini M. Surface motion upregulates superficial zone protein and hyaluronan production in chondrocyte-seeded three-dimensional scaffolds. *Tissue Eng.* 2005;11(1–2):249–256. doi:10.1089/ten.2005.11.249.
67. Kock LM, Ito K, van Donkelaar CC. Sliding indentation enhances collagen content and depth-dependent matrix distribution in tissue-engineered cartilage constructs. *Tissue Eng Part A.* 2013;19(17–18):1949–1959. doi:10.1089/ten.tea.2012.0688.
68. Khoshgoftar M, van Donkelaar CC, Ito K. Mechanical stimulation to stimulate formation of a physiological collagen architecture in tissue-engineered cartilage: a numerical study. *Comput Methods Biomech Biomed Eng.* 2011;14(2):135–144. doi:10.1080/10255842.2010.519335.